Al-containing MCM-41 type materials prepared by different synthesis methods: Hydrothermal stability and catalytic properties

J.P. Lourenço[*1], A. Fernandes[2], C. Henriques[2], M.F. Ribeiro[2]

[1] Universidade do Algarve, Faculdade de Ciências e Tecnologia, Departamento de Química e Bioquímica, Campus de Gambelas, P-8005-139 Faro, Portugal. e-mail:jlouren@ualg.pt.

[2] Instituto Superior Técnico, Departamento de Engenharia Química, Av. Rovisco Pais, P-1049-001 Lisboa, Portugal.

* Corresponding author.

Abstract

Al-containing MCM-41 type materials were prepared by three different synthesis methods (aluminum grafting on the calcined MCM-41, pH adjustment during the crystallization period and crystallization in the presence of zeolite seeds). The samples were characterized by powder XRD, nitrogen adsorption, ^{27}Al MAS NMR and FTIR with pyridine as probe molecule. All the samples exhibit a high hydrothermal stability at high temperature just with a minor structural degradation. N_2 adsorption data obtained for the sample prepared from a gel containing zeolite seeds suggest a higher structural resistance to the hydrothermal treatment in comparison with the samples prepared by other methods. A different type of pyridine adsorbed, probably interacting simultaneously with a Brönsted and a Lewis acid site, is observed upon pyridine adsorption. This type of adsorption is stronger for the sample prepared in the presence of zeolite seeds and is not observed on Al-grafted MCM-41.

The catalytic activity towards the isomerization of α-pinene depends mainly on the number of Brönsted acid sites. The data obtained in this study strongly indicate that for this type of materials, the Lewis acid sites do not influence the selectivity for the isomerization products.

Keywords: MCM-41, synthesis, hydrothermal stability, catalytic activity, α-pinene

1. Introduction

The discovery of the MCM-41 family of materials in the early 90's by Mobil researchers [1,2] rapidly led to a significant growth in the research activities on mesoporous solids. This new class of materials, with its ordered system of channels, high surface area and pore dimensions that can be tailored between ca. 15 to greater than 100 Å, shows a wide range of potential applications as catalysts in reactions with large molecules that can not enter into the pores of classical zeolites. Additionally, these materials may be used as support for the immobilization of organic functional groups and inorganic or organometallic complexes that can act as catalysts [3-9].

In spite of the interesting properties of these materials, soon it was observed that its thermal and hydrothermal stabilities are strongly dependent on the synthesis method.

Corma et al.[10] tested a series of MCM-41 with Si/Al ratio in the range 14-143 in vacuum gas oil cracking reactions and concluded that the calcined samples could be interesting for the conversion of large molecules, but, when a steaming treatment simulating the regeneration procedure of an FCC catalyst was carried out, the structure of the materials collapsed and the activity was strongly reduced.

To overcome the lack of stability of the original MCM-41, several strategies have been reported [11]. Some of them are based on the modification of the synthesis method such as adding salts to the synthesis gel to facilitate the condensation of silanol groups [12], pH

adjustment during the crystallization period [13,14], generating microporous zeolites - mesoporous composites in order to get advantage of the thermal stability and acidity of the zeolites [15,16] and using templates different from those of original MCM-41, such as triblock copolymer surfactants (which allow the preparation of mesoporous structures with thicker walls (ex. SBA-15) [17,18]) or Gemini amine surfactants for the preparation of vesicle-like lamellar frameworks with thick walls and improved hydrothermal stability [19]. Another promising strategy to achieve a good thermal and hydrothermal stability associated to a good acidity is the use of nanoclustered zeolite seeds as framework precursors. Several mesoporous materials, such as MSU-S [20, 21], MAS-7 [22], MAS-9 [23], MAS-3 and MAS-8 [24] have been reported using this approach.

Several post-synthesis treatments may also improve the stability of the mesoporous structures. One example of this type of treatments is the recrystallization of a primary MCM-41 structure which enhances the thermal stability by thickening the walls [25]. Additionally, the extraction of the template using acidic media prior to calcination has been reported to have a positive effect on the thermal stability of Al-MCM-41 [26].

This paper describes a comparative study of the thermal and hydrothermal stability of Al-containing MCM-41-type materials prepared by different synthesis methods: salt addition and pH adjustment during the crystallization period followed by aluminum grafting on the calcined sample, pH adjustment during the crystallization period and MSU-S material prepared from ZSM-5 seeds. The catalytic activity for acid catalyzed reactions was evaluated using the isomerization of α-pinene as model reaction.

2. Experimental

Synthesis

The synthesis of MCM-41 was carried out by first preparing the primary silica MCM-41 following closely the method reported by Kim et al. [12]. First, 144.3 g 1M NaOH solution (Merck) was mixed with 43.5 g Ludox HS-40 (DuPont, 40 wt% SiO_2) at 75 ºC for 1h. This solution was slowly added under vigorous magnetic stirring (at room temperature) to a mixture of 96.0 g hexadecyltrimethylammonium chloride (HTACl) (Aldrich, 25% aq. sol.) and 298.0 g of water. Stirring was maintained for an additional hour after the addition was completed. The final gel composition was 1 SiO_2 : 0.25 Na_2O : 0.25 HTACl : 100 H_2O.

The gel was then introduced into a polypropylene bottle and kept in an oven at 100 ºC for 24 h. The reaction mixture was cooled to room temperature, the pH was adjusted to 10 using acetic acid (Riedel-deHaen) and the bottle replaced into the oven. After 24 h, 13.0 g NaCl (Merck, p.a.) were added to the gel and the bottle kept in the oven for 10 days. After this period, the pH was adjusted one more time following the same procedure. The product was centrifuged, washed with distilled water and dried at 80 ºC overnight.

The template was partially removed by extraction with a solution 0.1M NH_4NO_3 (Merck) in 96% ethanol at reflux temperature for 2 h. After drying, the product was calcined under a flux of dry air at 550 ºC for 10 h. The temperature was increased from 25 to 550 ºC at 1ºC/min.

To prepare the Al-grafted MCM-41, a solution containing 8.4 g $AlCl_3.6H_2O$ (Aldrich, 99.8%), 42.0 g H_2O and 53.4 g tetramethylammonium hydroxide (TMAOH, Fluka, 10% aq. sol.) was prepared under stirring at 80 ºC. This solution was mixed with 2.0 g of calcined MCM-41 and kept under stirring for 2 h. After centrifugation and washing, the product was dried at 80 ºC overnight and then calcined at 450 ºC under dry air for 5 h.

The direct preparation of AlMCM-41 followed the method described by Lindlar et al. [14]. A mixture of 106.5 g sodium silicate solution (Riedel-deHaen, pure), 2.85 g Cab-osil M5

(Riedel-deHaen) and 178.0 g of deionized water was slowly added to a mixture of 84.25 g HTACl and 1.4 g ammonium hydroxide solution (Merck, 25%). Then, a solution of 1.25 g sodium aluminate (Riedel-deHaen) in 6.5 g deionized water was added dropwise. The final molar composition of the gel was 1 SiO_2 : 0.013 Al_2O_3 : 0.277 Na_2O : 0.126 HTACl : 0.019 NH_3 : 33.7 H_2O. The gel was kept under magnetic stirring for 1 h and then heated at 100ºC for 24 h under static conditions (in a polypropylene bottle). After this period, the product was cooled to room temperature and the pH was adjusted to 11 using acetic acid. The bottle was replaced into the oven at 100 ºC and the procedure was repeated twice. The recovery of the final product and removal of template followed the same procedure described above.

The sample of MSU-S (MSU-S(MFI)) was prepared as described by Liu et al. [21]. The zeolite MFI seeds were formed from the reaction of 20.49 g of tetrapropylammonium hydroxide (TPAOH, Fluka, 20% aq. sol.), 0.34 g sodium aluminate, 6.0 g Cab-osil M5 and 69.0 g of deionized water, at 50 ºC for 18 h under stirring. Then, 9.44 g hexadecyltrimethylammonium bromide (HTABr) (Fluka) and 100 g of deionized water were added to the seeds suspension. The final molar gel composition was 1 SiO_2 : 0.018 Al_2O_3 : 0.023 Na_2O : 0.266 HTABr : 0.2 TPAOH : 103.6 H_2O.

After mixing, the gel was heated (in a teflon-lined autoclave) at 150 ºC for 2 days. The recovery of the final product and removal of template followed the same procedure described above for the preparation of the silica MCM-41.

Steaming treatments

For the evaluation of the hydrothermal stability, the calcined samples were heated under air saturated with water (25 ºC) at 10 ºC/min from room temperature to 800 ºC and maintained at this temperature for 12 h.

Characterization

Powder XRD patterns of as-synthesized, calcined and steamed samples were recorded on a Rigaku diffractometer using CuKα radiation filtered by Ni. The composition of the samples was determined by bulk chemical analysis (ICP and AAC). Nitrogen adsorption of the calcined and steamed samples was measured at -196 ºC with an ASAP 2010 Micromeritics apparatus. Prior to the measurements, the samples were degassed at 350ºC for 3 h. The specific surface area was estimated by the BET method, and for the pore diameter, it was considered the average pore diameter determined by the relation $4V_{mes}/S_{BET}$, where V_{mes} is the mesoporous volume estimated from the N_2 adsorption isotherms and the surface area, S_{BET}, calculated considering the area covered of a N_2 molecule as 13.5 $Å^2$ according to recent proposals [27, 28] .

Thermogravimetric measurements were performed on a TG-DTA/DSC LABSYS-SETARAM under air at a heating rate of 10º/min

^{27}Al MAS NMR spectra were recorded on a Bruker Avance 400 spectrometer at 104.3 MHz, using short and powerful radio-frequency pulses (0.6 μs equivalent to 10º pulse angle), spinning rates of 14-15 kHz and a recycle delay of 1 s. Chemical shifts are quoted in ppm from $Al(H_2O)_6^{3+}$.

The acid sites of the various samples were characterized by FTIR, using pyridine as probe molecule. The self-supported wafers (~6 mg cm^{-2}) were treated under vacuum (1.33 x 10^{-4} Pa) at 300 ºC for 3 h prior to contact with pyridine (400 Pa) at room temperature. The system was outgassed for 15 min at room temperature before the heating treatment of the wafer at 150, 200, 250, 300 and 350 ºC. A spectrum was recorded for each temperature after outgassing for 15 min. Band intensities were normalized by the sample weight. The background spectrum, recorded under identical operating conditions without sample, was always performed before each spectrum and automatically subtracted.

Catalytic tests

The isomerization of α-pinene was carried out at 50 ºC or 80 ºC using toluene as solvent. For each catalytic test, 10 mL toluene (Aldrich) and 1 mL α-pinene (Aldrich, 98 %) were introduced into a two necked flask equipped with a condenser and a rubber septum. The reaction was started with the introduction of 100 mg of catalyst. Before introduction into the reaction mixture, all the catalysts were activated for 3 h at 450 ºC under nitrogen.

Periodically, small aliquots of the reaction mixture were analyzed by gas chromatography on a Chrompack CP9001 chromatograph equipped with a Macherey-Nagel Optima-5 column. The identification of the products was achieved by injecting standard products and by GC-MS analysis of selected samples on a HP 5890 SERIES II equipped with the same column and a 5971 series mass detector.

3. Results and discussion

Synthesis and characterization

The materials prepared by the different methods described above show XRD patterns similar to that of typical MCM-41. Fig. 1 shows that after template removal, the mesoporous materials retain the long-range hexagonal order.

The sample MCM-41 exhibits four distinct diffraction peaks that can be indexed as (100), (110), (200) and (210) in the hexagonal symmetry revealing the high structural organization of the mesoporous structure. The grafting of aluminum on the pore walls of this material modifies, in some extent, the periodicity of hexagonal pore system. However, upon the grafting procedure (sample Al-MCM-41 graf.) the hexagonal structure is maintained as indicated by the XRD pattern where three diffraction peaks are clearly visible.

The XRD patterns of MSU-S(MFI) and in less extent that of AlMCM-41 are less resolved than those of the silica counterpart, due to the presence of less flexible aluminum

environments that may cause local distortions and consequently some broadening of diffraction peaks. It is interesting to note that the XRD pattern of MSU-S(MFI) is characteristic of a less ordered structure than that reported by Liu et al. [21], although the synthesis method reported by these authors had been followed. Alternatively to the hypothesis of a less ordered structure, a small crystallite size may also be considered to explain the shape of the XRD pattern.

The nitrogen adsorption isotherms (Fig. 2) are typical of mesoporous structures (type IV). With exception of the sample Al-MCM-41 graf., the presence of pore filling steps within a narrow range of p/p_o along with the reversibility of the step is consistent with the presence of tubular pores of uniform size [27, 28].

The structural characteristics, after template removal (calcined samples), are compared in Table 1. For determination of the pore diameter of mesoporous materials (Dp) it has been reported that some methods as the BJH, although widely used, do not allow an accurate estimation of this parameter [27,28]. In this paper, we used the Gurvitsch method, $D_p= 4V_p/S$ (where V_p stands for porous volume and S for surface area). To obtain more accurate results, the surface area (BET) was estimated considering the area covered by a N_2 molecule as 13.5 $Å^2$ and the volume of the mesoporous (V_{mes}) was obtained from the N_2 adsorption isotherm at the top of the adsorption step as proposed by Galarneau et al. [27].

The values of Table 1 show that the grafting of aluminum on the surface of MCM-41 leads to, as expected, a decrease of both surface area and pore diameter compared to the parent material. This is not necessarily an indication of pore structure degradation but it should be rather due to the deposition of the aluminum on the internal walls of the pores. Additionally and also in line with the deposition of aluminum on the surface walls an increase of the wall thickness is observed.

The samples AlMCM-41 and MSU-S(MFI) show similar surface areas and pore diameters, but the latter material exhibits a slightly thicker pore wall.

Upon template removal, the samples AlMCM-41 and MSU-S(MFI) exhibit a main peak in the ^{27}Al NMR spectra at ca. 52 ppm and a less intense but significant broad band around 0 ppm, which are usually assigned to tetrahedral and octahedral aluminum coordinations, respectively (Fig. 3A). The latter band may be decomposed at least in two peaks: one sharp with maximum at 0 ppm and a broader one with maximum at ca. -15 ppm. In addition, the presence of distorted tetrahedral or five-coordinated aluminum can not be discarded due to the signal intensity observed around 30 ppm [29,30].

The presence of six-coordinated aluminum (NMR band with maximum at ca. 0 ppm) in these samples may be due to a slight dealumination process that occurs during the template removal or to the presence of some aluminum sites that are grafted to the structure and complete their coordination with water molecules or OH groups [26]. The lack of a rigid structural organization of the walls, typical of this type of materials, probably favors the presence of aluminum sites with those characteristics. It should be noted that no special precautions were taken for the NMR measurements and thus the samples were equilibrated with atmospheric air. Therefore it is reasonable to consider the presence of adsorbed water that can complete the hexacoordination of some aluminum sites.

The spectrum of calcined Al-MCM-41 graf. (Fig. 3A) exhibits a complex and wide distribution of the coordinations of aluminum. Due to its complexity, the complete characterization of the aluminum species requires advanced NMR techniques which are not the aim of this paper. Nevertheless, it can be seen that along with the peaks typical of tetrahedral and octahedral aluminum (53 ppm and 0 ppm, respectively) at least two other peaks with maxima at ca. 30 ppm and 13 ppm are clearly visible. These resonances may be assigned to pentacoordinated and hexacoordinated aluminum sites respectively. The presence

of different aluminum coordinations upon grafting with aluminum isopropoxide was also reported by Anwander et al. [29]. This distribution of aluminum sites reflects the multiple possibilities of grafting aluminum atoms due to the distribution of OH groups at the surface of the walls.

FTIR spectra of pyridine adsorbed on aluminum-containing samples, recorded after outgassing at 150 ºC, are displayed in Fig. 4A (150 ºC). The spectra display bands at 1547 and 1639 cm^{-1} assigned to pyridine adsorbed on Brönsted acid sites, bands at 1454 and 1621 cm^{-1} assigned to pyridine adsorbed on Lewis acid sites and a band at 1491 cm^{-1} characteristic of pyridine adsorbed on both sites [31]. The spectra of AlMCM- 41 and MSU-S(MFI) show further bands at 1445 and 1598 cm^{-1} that have been assigned to H-bonded pyridine [31] or to a pyridine molecule adsorbed on a Lewis acid site and interacting through hydrogen bonding with a protonic site [32].

The spectrum of pyridine adsorbed on MCM-41, recorded after outgassing at room temperature (not shown) just shows the set of bands assigned to H-bonded pyridine (bands at 1445 and 1598 cm^{-1}). These bands completely vanish at 150 ºC, as expected for weak adsorption sites.

The spectra recorded after outgassing at 300 ºC (Fig. 4A (300ºC)) shows the same set of bands due to pyridine molecules that remain adsorbed on Brönsted and Lewis acid sites. The presence of pyridine molecules adsorbed at this temperature indicates the presence of acid sites at least with moderate strength. It is interesting to note that the set of bands at 1445 and 1598 cm^{-1} vanish at 300 ºC in the spectrum of AlMCM-41 but remain in the spectrum of MSU-S(MFI).

Marques et al. [32], working with dealuminated BEA zeolites, observed for temperatures above 350 ºC the appearance of a band generally ascribed to iminium ions (1462 cm^{-1}), apparently at the expense of the bands at 1446 and 1603 cm^{-1}. The authors explain this

observation on the basis of the formation of an iminium ion by protonation of the pyridine molecule adsorbed on the Lewis acid site. In the present work, no band at ca. 1462 cm^{-1} has been observed, however, this is not in contradiction with the assignment made by these authors if one considers that the strength of the acid sites is lower in this class of mesoporous materials than in dealuminated BEA zeolite. Indeed, if the acid sites are not strong enough, the pyridine molecule could interact simultaneously with a Lewis and a Brönsted acid site as described in [32] but will not be protonated to give the iminium ion. Nevertheless, the possibility of this type of interaction with other molecules could have a significant effect on the catalytic activity of the material. This effect should be more pronounced on MSU-S(MFI) since this type of pyridine remains adsorbed at higher temperature.

Steaming treatment

The samples were submitted to a steaming treatment at 800 ºC in order to study their hydrothermal stability, which can be an important parameter to be considered if these materials would be applied as catalysts in reactions where water is produced or need to be regenerated in the presence of water vapor.

After the treatment, the samples retain a high hexagonal order, in spite of the slight cell contraction, as indicated by the XRD results (Fig. 1 and Table 1). The N_2 adsorption measurements show for all the steamed samples a decrease both the surface area and average pore size (Table 1). Nevertheless, the data indicate that the sample MSU-S(MFI) is somewhat more resistant to the hydrothermal treatment than the other samples: upon the treatment it loses less surface area and shows a lower decrease in the average pore diameter as well. Even if this sample exhibits a XRD pattern typical of a less ordered structure, this higher resistance suggests that the synthesis method may have allowed the formation of MFI zeolite precursors which certainly have a positive effect on the stability. Liu et al. [21] reported the presence of a

band at about 570 cm^{-1} in the IR spectra of MSU-S materials synthesized with ZSM-5 and BEA zeolite seeds. The authors concluded that the presence of this band, characteristic of five-membered ring subunits, was an indication of the presence of zeolite microdomains. In the present work this band is present in the spectra of all samples, however, the intensity is higher for the sample MSU-S(MFI) (Fig. 5) which is in line with the presence of MFI microdomains and consequently with the higher stability.

Fig. 3B displays the ^{27}Al NMR spectra recorded after the steaming treatment. The spectra of AlMCM-41 and MSU-S(MFI) are very similar, suggesting that the same changes occur for both materials under this treatment. When compared with the spectra recorded before the steaming treatment a significant decrease of the peak at 53 ppm (assigned to tetrahedral aluminum) and the appearance of resonances at 13 ppm and at ca 30 ppm (shoulder) are observed. The peak at 0 ppm assigned to octahedral aluminum seems to decrease; however, a broad band at lower frequency still remains in the spectra. The appearance or increase of the peaks at 13 and 30 ppm may result from the hydrolysis (complete or incomplete) of Al-O-Si bonds. This process certainly gives rise to new coordinations for some aluminum sites even if the aluminum atoms are not completely extracted from the structure. These aluminum sites should be similar to those reported by Hitz and Prins [26] who found that Al-containing MCM-41 may have a substantial amount of flexible aluminum sites that can change their coordination number depending on the chemical environment.

The spectrum of Al-MCM-41 graf. recorded after the steaming treatment does not show drastic changes. The relative intensities of the peaks with maxima located at 13 and 30 ppm increase with respect to the peaks at 53 and 0 ppm. The broadness of the peaks is probably a consequence of the large distribution of environments for aluminum sites. It sould be noted that before the hydrothermal treatment the material already had a wide distribution of aluminum coordinations.

Adsorption of pyridine on steamed samples (Fig. 4B) reveals the presence of both Brönsted and Lewis acid sites, even though a decrease in the band intensities is observed when compared with the calcined parent materials. A decrease of the amount of acid sites should be expected, since the decrease of surface area may have caused some pore blockage and consequently a reduction of the number of acid sites accessible to the pyridine. Moreover, under these drastic conditions the amount of octrahedrally coordinated aluminum has increased as indicated by NMR data and therefore this also contributes to the reduction of acid sites.

The hydrothermal treatment had a stronger effect on the surface properties of MSU-S(MFI): after steaming, the spectra of this sample do not show the set of bands at 1445 and 1598 cm^{-1} anymore. Along with this effect, the treatment also had a stronger effect on the amount of moderate and strong Brönsted acid sites of that sample since the bands due to pyridine adsorbed on Brönsted acid sites almost vanish after outgassing at 300 ºC. The decrease of the amount of Brönsted acid sites may be explained by the migration of aluminum atoms (formerly tetrahedral in the MFI microdomains) to the outer surface of microcrystals, which turn into perfectly octahedrally coordinated Al that do not induce acid sites [33].

Catalytic tests

The conversion of α-pinene in the conditions described above, produces mainly camphene, limonene, α-terpinene, γ-terpinene, terpinolene and in some cases a small amount of p-cymene. All the compounds other than camphene and limonene are likely to be produced by the same pathway that gives limonene and/or from the conversion of limonene itself, as indicated in Fig. 6.

The catalytic activity and selectivity shown by the different samples are summarized in Table 2 (only the selectivity for the main products is reported). The monocyclic/bicyclic ratio was

defined as the sum of the yields of limonene, α-terpinene, γ-terpinene, terpinolene and p-cymene divided by the yield of camphene.

The less active catalyst, MCM-41, does not exhibit a significant activity at 50 ºC, however, when the temperature is raised to 80 ºC the conversion of α-pinene increases and reaches ca. 17 % at 20 min. The ability of a siliceous mesoporous structure similar to MCM-41 (FSM-16), to catalyze the isomerization of α -pinene was already reported by Yamamoto et al. [31]. These authors explain the activity of the catalyst on the basis of the presence of weakly perturbed vicinal pairs of silanol groups. Since in the present work the adsorption of pyridine did not evidence the presence of Brönsted or Lewis acid sites, it seems reasonable to assume that the same type of silanol groups are responsible for the activity of this material.

The samples with aluminum show different activities for the isomerization depending on the preparation method. The grafting of aluminum on MCM-41 increases the activity of the material (the sample Al-MCM-41 graf. shows higher activity at 50 ºC than the sample MCM-41 at 80ºC). Nevertheless, the activity is still low when compared with the samples AlMCM-41 and MSU-S(MFI) with higher Si/Al ratios. MSU-S(MFI) shows higher activity than AlMCM-41 as indicated by the higher conversion of α-pinene after 2 min of reaction.

Table 3 shows the number of acid sites estimated by pyridine adsorption according to Emeis [34]. For the calculations we have assumed that the value of the integrated molar extinction coefficient for the band at 1545 cm^{-1} due to pyridine adsorbed on a Brönsted acid site is 1.67 cm/μmol and that for the band at 1455 cm^{-1} due to pyridine adsorbed on a Lewis acid site is 2.22 cm/μmol. Additionally we have also assumed that these integrated extinction coefficients do not change with the acid strength [34].

The amount of Brönsted acid sites with moderate strength (Table 3) may explain the higher activity of MSU-S(MFI) when compared with AlMCM-41 (Fig 7). Nevertheless it can not be excluded that the possibility of having species simultaneously interacting with Brönsted and

Lewis acid sites as suggested from pyridine adsorption, may also increase the catalytic activity.

This simple analysis based on the number of acid sites, does not explain the lower activity of Al-MCM-41 graf. In this case, it is possible that the thermal treatment carried out before the catalytic test aiming at the decomposition of the aluminum precursor was not efficient. Consequently some aluminum could remain partially coordinated to the original ligands (mainly OH^-) and may not contribute to the generation of active sites. In order to check the efficiency of the pre-treatment on this sample, a thermogravimetric analysis was performed and the results are presented in Fig. 8. A first weight loss occurs below 200 ºC due to desorption of water and other weakly adsorbed species. A small weight loss is also observed in the range 400 – 550 ºC probably due to the decomposition of the aluminum precursor. On the other hand, a new catalytic test was carried out with a sample calcined for 10 h at 550 ºC but the catalytic activity is very similar to that observed with the sample previously calcined at 450ºC, showing that the pretreatment at 550ºC under dry atmosphere did not lead to an improvement of the Al reorganization, with a consequent generation of acid sites. However, this occurrence was detected when the pretreatment is performed under wet air, as it will be shown hereafter. Moreover it is also possible to envisage that the pre-treatment under high vacuum carried out before pyridine adsorption might have some effect on the reorganization of Al species on the surface. So, in this particular case of Al-MCM-41 graf. sample, the amount of acid sites estimated by pyridine adsorption does not correlate with the catalytic activity possibly due to different surface properties imposed by the different pre-treatments (calcination, steaming or vacuum).

Concerning the selectivity it should be noted that due to the characteristics of this type of materials (regular array of pores with a large diameter) any selectivity imposed by the

structure is not expected. The differences observed should be mainly an effect of the different distribution and strength of the acid sites.

The formation of other products than camphene and limonene occurs for all the catalysts. The increase of the α-pinene conversion does not significantly change the selectivity. A small increase of limonene selectivity is observed for the less active samples and a small decrease for the most active ones. At high conversion of α-pinene, limonene converts more rapidly to α-terpinene, γ-terpinene and terpinolene and so it justifies the small increase in the camphene selectivity and small decrease in limonene selectivity.

Severino et al. [35], using FAU type zeolites, correlated the selectivity to camphene with the presence of Lewis acid sites. In the present study it was not possible to confirm this conclusion. The selectivity to camphene obtained with MCM-41 is similar to that obtained with the other samples that have Lewis acid sites. Further, a comparison of Table 2 with Table 3 clearly shows that the samples with a high Lewis/Brönsted ratio do not have necessarily a high selectivity to camphene. Therefore, the data presented in Tables 2 and 3 are better explained if the main active sites for this reaction are the Brönsted acid sites, since the changes in the number of Lewis acid sites do not seem to influence the selectivity. These results are well in line with the conclusions of Yamamoto et al. for FSM-16 [31] and Gunduz et al. [36] for BEA zeolite.

The steaming treatment, as pointed above, may cause dealumination by a process similar to the one that occurs in zeolites. This process is expected to bring about a reduction of the number of Brönsted acid sites creating extra-framework aluminum [37] or at least the hydrolysis of some bonds changing the coordination of aluminum sites, as suggested by the changes in the ^{27}Al NMR spectra. Along with this process, also the partial degradation of the structure has influence on the measured acidity and catalytic activity since it can block the accessibility of molecules to a part of potential active sites.

For the materials under study, the number of acid sites was drastically decreased upon the hydrothermal treatment (Table 3). This decrease is more evident for Lewis acid sites than for Brönsted acid sites, except for the sample MSU-S(MFI) where the opposite behavior was observed.

The analysis of Table 2 and Fig. 9 shows that after steaming, the Al-MCM-41 graf. sample manifests an important increase of activity, which is more evident after 20 min of reaction. This behavior may be explained by a reorganization of aluminum species leading to the migration of aluminum atoms into the walls of the mesoporous material and thus generating active sites.

The steamed AlMCM-41 evidences a slight decrease of α-pinene conversion, which is more evident in the case of MSU-S(MFI), for which the steaming treatment clearly leads to a decrease of catalytic activity (a conversion reduction of about 60% was observed at 20 min of reaction). The reduction of the number of Brönsted acid sites observed on this sample during the steaming seems to be responsible for this reduction of activity (Fig. 7). The selectivity is similar to that obtained with the calcined samples. The high Lewis/Brönsted ratio of the sample MSU-S(MFI) does not seem to influence the selectivity. This fact confirms that the Lewis acid sites do not play an important role in the catalytic process with this type of materials.

4. Conclusion

All the synthesis methods that were tested allow the preparation of thermal and hydrothermal stable mesoporous materials. The samples prepared for this study can be submitted to hydrothermal treatments at high temperatures without a significant loss of structural organization. The higher activity observed for the sample MSU-S(MFI) and the small decrease of surface area and pore diameter after the hydrothermal treatment indicate that the

synthesis method with zeolite seeds allowed the preparation of a material with improved properties. The present work confirms that the presence of zeolite microdomains may increase the structural stability and also increases the acidity of mesoporous materials.

The results of the catalytic activity towards α-pinene isomerization have shown that the Brönsted acid sites play the major role in this process although the surface distribution of the Lewis and Brönsted acid sites could influence the activity. No evidence was found for a dependence of the selectivity on the amount of Lewis acid sites.

Acknowledgments

We thank Prof. João Rocha for providing the NMR spectra and Prof. Teresa Duarte for access to the XRD facility.

References

[1] - C.T. Kresge, M.E. Leonowicz, W.J. Roth, J.C. Vartuli, J.S. Beck, Nature, 359 (1992) 710.

[2] – J.S. Beck, J.C. Vartuli, W.J. Roth, M.E. Leonowicz, C.T. Kresge, K.D. Schmitt, C.T.-W.Chu, D.H. Olson, E.W. Sheppard, S.B. McCullen, J.B. Higgins, J.L. Schlenker, J.Am. Chem. Soc., 114 (1992) 10834.

[3] – H. Koch, W. Reschetilowski, Microporous Mesoporous Mater., 25 (1998) 127.

[4] – K. Möller, T. Bein, Chem. Mater., 10 (1998) 2950.

[5] – A.P. Wight, M.E. Davis, Chem. Rev., 102 (2002) 3589.

[6] – D.E. De Vos, M. Dams, B. F. Sels, P.A. Jacobs, Chem. Rev.,102 (2002) 3615.

[7] – D. Brunel, A.C. Blanc, A. Galarneau, F. Fajula, Catal. Today, 73, (2002) 139.

[8] – A. Corma, H. Garcia, A. Moussaif, M.J. Sabater, R. Zniber, A. Redouane, Chem. Commun., (2002) 1058.

[9] – H.M. Hultman, M. de Lang, I.W.C.E. Arends, U. Hanefeld, R.A. Sheldon, T. Maschmeyer, J. Catal., 217 (2003) 275.

[10] – A. Corma, M.S. Grande, V. Gonzalez-Alfaro, A.V. Orchilles, J. Catal., 159 (1996) 375.

[11] – Y. Liu, T.J. Pinnavaia, J. Mater. Chem., 12 (2002) 3179.

[12] – J.M. Kim, S. Jun, R. Ryoo, J. Phys. Chem. B, 103 (1999) 6200.

[13] – R. Ryoo, J.M. Kim, J. Chem. Soc. Chem. Commun., (1995) 711.

[14] - B. Lindlar, A. Kogelbauer, R. Prins, Microporous Mesoporous Mater., 38 (2000) 167.

[15] – A. Karlsson, M. Stöcker, R. Schmidt, Microporous Mesoporous Mater., 27 (1999) 181.

[16] – L. Huang, W. Guo, P. Deng, Z. Xue, Q. Li. J. Phys. Chem. B, 104 (2000) 2817.

[17] – D. Zhao, J. Feng, Q. Huo, N. Melosh, G.H. Frederickson, B.F. Chmelka, G.D. Stucky, Science, 279 (1998) 548.

[18] - D. Zhao, Q. Huo, J. Feng, N. Melosh, B.F. Chmelka, G.D. Stucky, J. Am. Chem. Soc., 120 (1998) 6024.

[19] – S.S. Kim, Y. Liu, T.J. Pinnavaia, Microporous Mesoporous Mater., 44 (2001) 489.

[20] – Y. Liu, W. Zhang, T.J. Pinnavaia, J. Am. Chem. Soc., 122 (2000) 8791.

[21] - Y. Liu, W. Zhang, T.J. Pinnavaia, Angew. Chem. Int. Ed. 40 (2001) 1255.

[22] – Y. Han, F.-S. Xiao, S. Wu, Y. Sun, X. Meng, D. Li, S. Lin, F. Deng, X. Ai, J. Phys. Chem. B, 105 (2001) 7963.

[23] - Y. Han, S. Wu, Y. Sun, D. Li, F.-S. Xiao, J. Liu, X. Zhang, Chem. Mater., 14 (2002) 1144.

[24] – Y. Di, Y. Yu, Y. Sun, X. Yang, S. Lin, M. Zhang, S. Li, F.-S. Xiao, Microporous Mesoporous Mater., 62 (2003) 221.

[25] – R. Mokaya, J. Phys. Chem. B, 103 (1999) 10204.

[26] – S. Hitz, R. Prins, J. Catal. 168 (1997) 194.

[27] – A. Galarneau, D. Desplantier, R. Dutarte, F. Di Renzo, Microporous Mesoporous Mater., 27 (1999) 297.

[28] – M.M.L. Ribeiro Carrott, A.J.E. Candeias, P.J.M. Carrott, P.I. Ravikovitch, A.V. Neimark, A.D. Sequeira, Microporous Mesoporous Mater., 47 (2001) 323.

[29] – R. Anwander, C. Palm, G. Gerstberger, O. Groeger, G. Engelhardt, Chem. Commun., (1998) 1811.

[30] – T.H. Chen, B.H. Wouters, P.J. Grobet, Eur. J. Inorg. Chem., 2 (2000) 281.

[31] – T. Yamamoto, T. Tanaka, T. Funabiki, S. Yoshida, J. Phys. Chem. B 102 (1998) 5830.

[32] – J.P. Marques, I. Gener, P. Ayrault, J.C. Bordado, J.M. Lopes, F. Ramoa Ribeiro, M. Guisnet, Microporous Mesoporous Mater., 60 (2003) 251.

[33] – T. Masuda, Y. Fujikata, S.R. Mukai, K. Hashimoto, Appl. Catal. A: General, 172 (2000) 73.

[34] – C.A. Emeis, J. of Catal., 141 (1993) 347.

[35] – A. Severino, A. Esculcas, J. Rocha, J. Vital, L.S- Lobo, Appl. Catal. A: General 142 (1996) 255.

[36] – G. Gunduz, R. Dimitrova, S. Yilmaz, L. Dimitrov, Appl. Catal. A: General 282 (2005) 61.

[37] – J. Scherzer, ACS Symp. Ser., 248 (1984) 157.

Figure captions

Figure 1. XRD patterns of the mesoporous structures recorded after template removal and steam treatment.

Figure 2. Nitrogen adsorption isotherms after template removal.

Figure 3. ^{27}Al MAS NMR spectra recorded after calcination (A) and after the steaming treatment (B): (a) AlMCM-41, (b) MSU-S(MFI) and (c) Al-MCM-41 graf.

Figure 4. Difference FTIR spectra (mass corrected) upon pyridine adsorption on calcined (A) and steam treated (B) samples, outgassed at 150 ºC and 300 ºC: (a) AlMCM-41, (b) MSU-S(MFI) and (c) Al-MCM-41 graf.

Figure 5. FTIR spectra of calcined MCM-41 (a) and MSU-S(MFI) (b).

Figure 6. Scheme for α-pinene isomerization over MCM-41-type materials.

Figure 7. Catalytic conversion of α-pinene at 2 min. of reaction *versus* number of Brönsted acid sites ((◊♦) Al-MCM-41-graf, (□■) AlMCM-41, (Δ▲) MSU-S(MFI)). The black symbols correspond to the calcined samples and the white symbols to the steam treated samples.

Figure 8. TG/DTA diagrams of Al-MCM-41 graf.

Figure 9. Catalytic activity for the isomerization of α-pinene before (♦) and after (▲) the steaming treatment.

Table 1. Structural characteristics of the mesoporous structures after template removal and steam treatment.

Sample		Si/Al	a_o (Å)[(a)]	S_{BET} (m^2/g)	D_p (Å)[(b)]	W.t. (Å)[(c)]
MCM-41	(calc.)	---	48.7	837	39.3	11.4
	(st)		44.7	800	35.0	
Al-MCM-41(graf)	(calc.)	13	46.9	706	35.6	13.1
	(st)		41.2	525	29.4	
AlMCM-41	(calc.)	30	48.0	881	38.3	11.6
	(st)		43.4	669	32.2	
MSU-S(MFI)	(calc.)	24	49.9	873	38.4	13.4
	(st)		48.3	710	35.6	

(a) determined for a hexagonal symmetry as $a_o = 2d_{100}/\sqrt{3}$.

(b) $D_p = (4V_{mes}/S_{BET})$, taking the correction for S_{N_2}=13.5 $Å^2$ [27].

(c) wall thickness determined as: W.t.= a_o-0.95D_p [27].

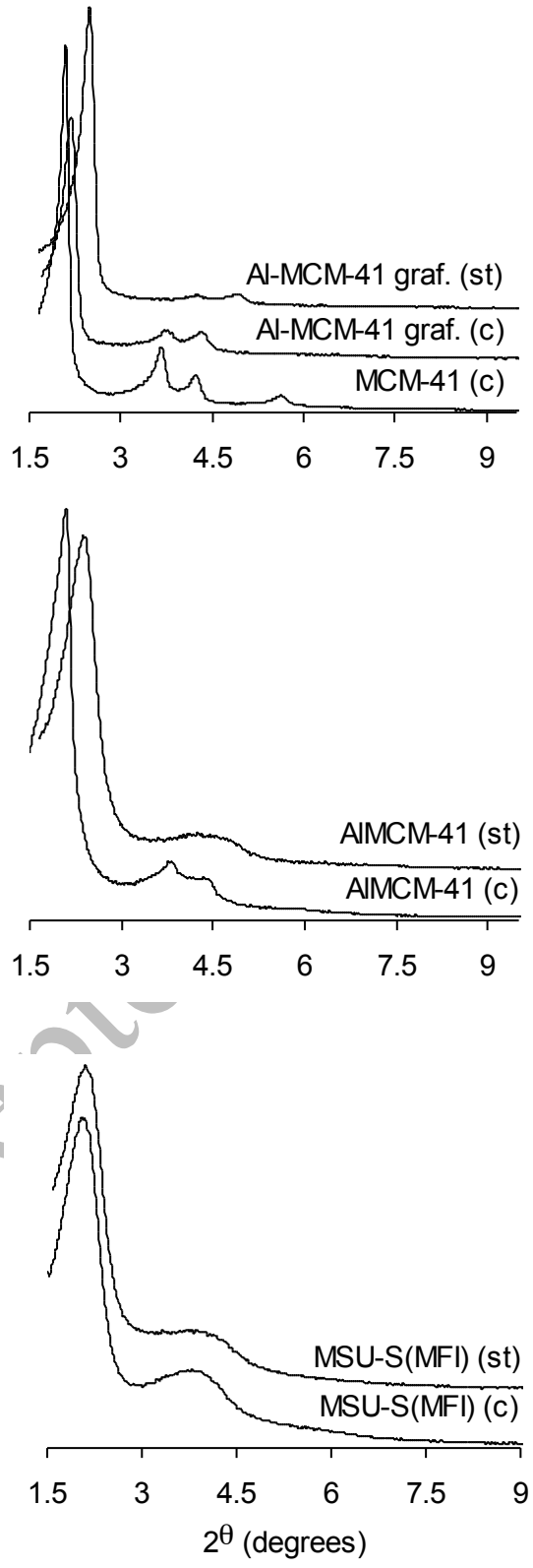
Al-MCM-41 graf. (st)
Al-MCM-41 graf. (c)
MCM-41 (c)
1.5
3
4.5
6
7.5
9
AlMCM-41 (st)
AlMCM-41 (c)
1.5
3
4.5
6
7.5
9
MSU-S(MFI) (st)
MSU-S(MFI) (c)
1.5
3
4.5
6
7.5
9
2θ (degrees)

Figure 1.

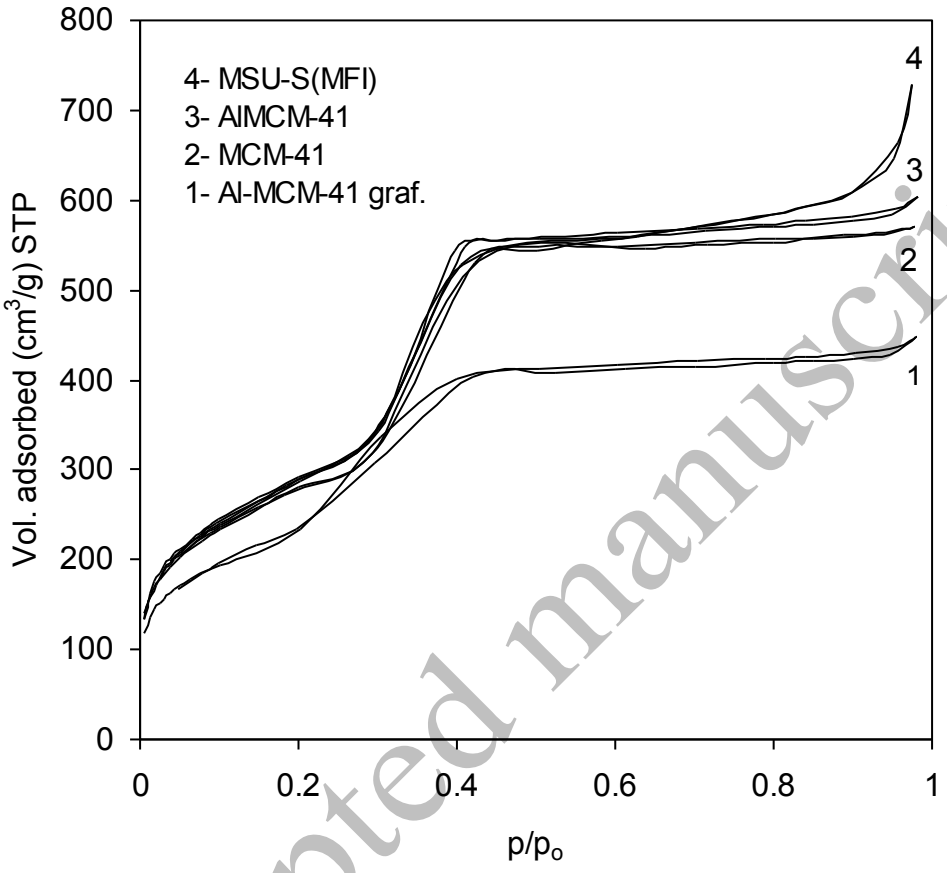

Figure 2.

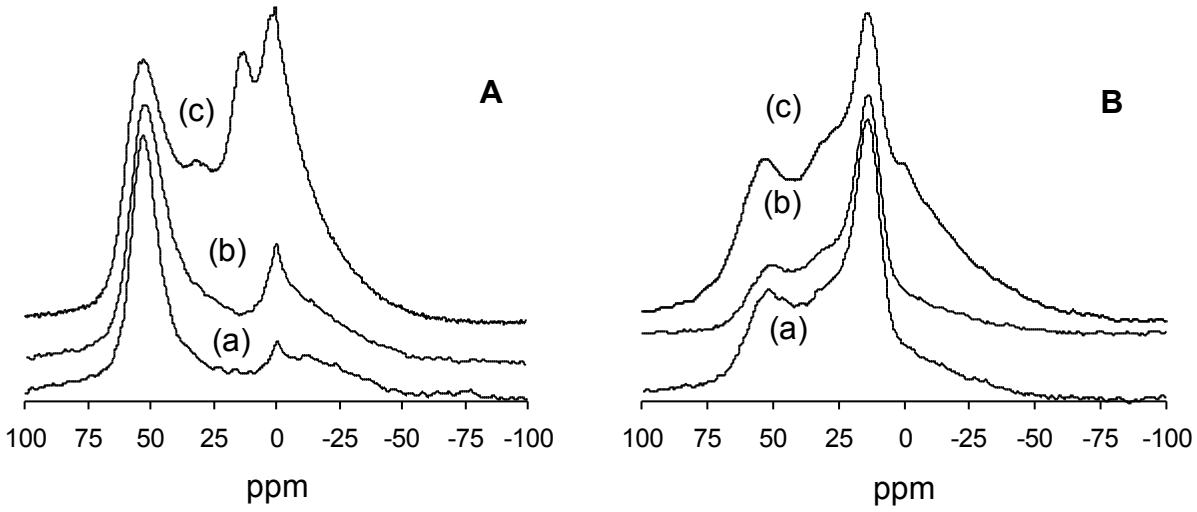

Figure 3

J.P. Lourenço et al.
"Al- containing MCM-41 …"

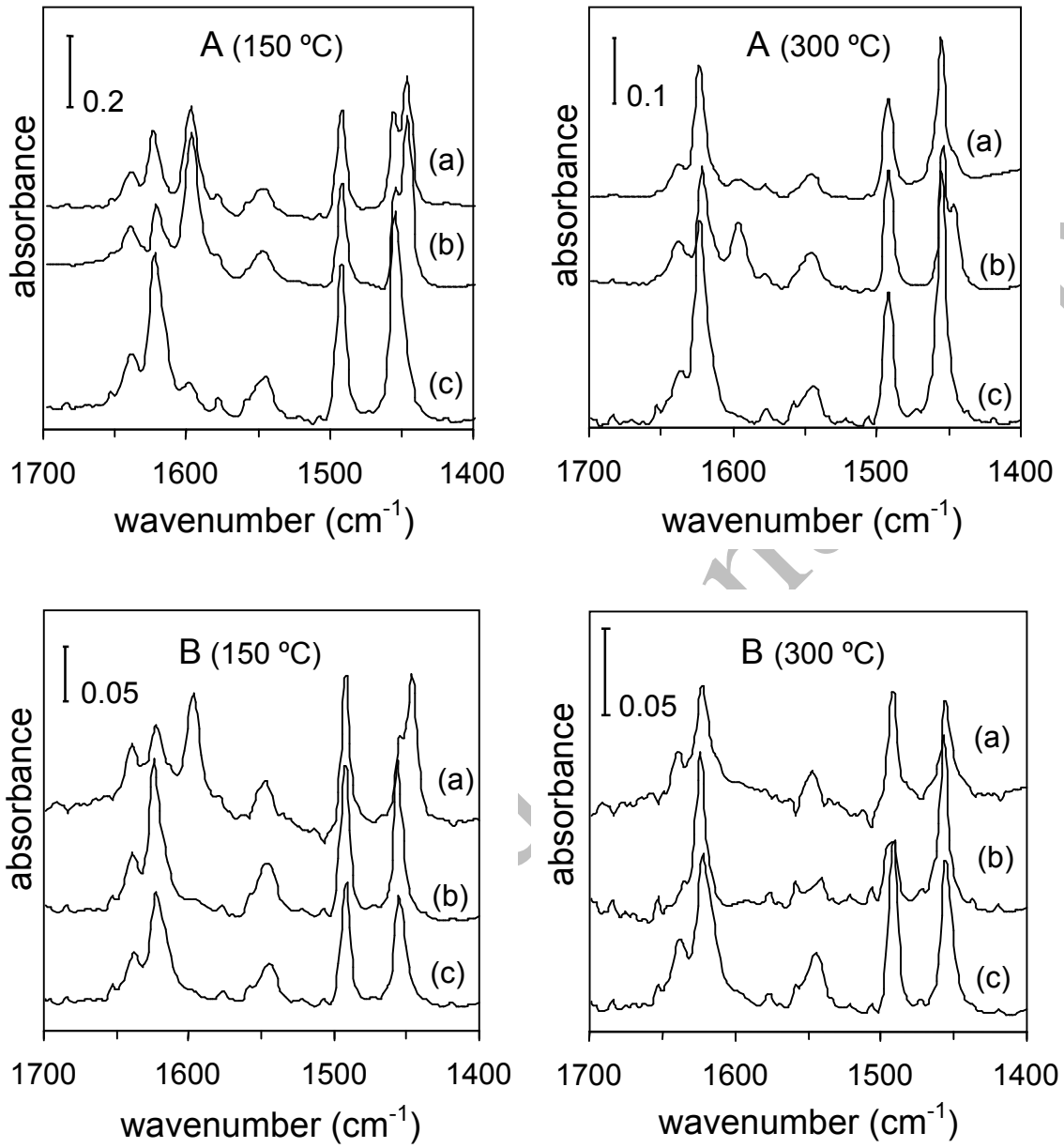

Figure 4.

J.P. Lourenço et al.
"Al- containing MCM-41 …"

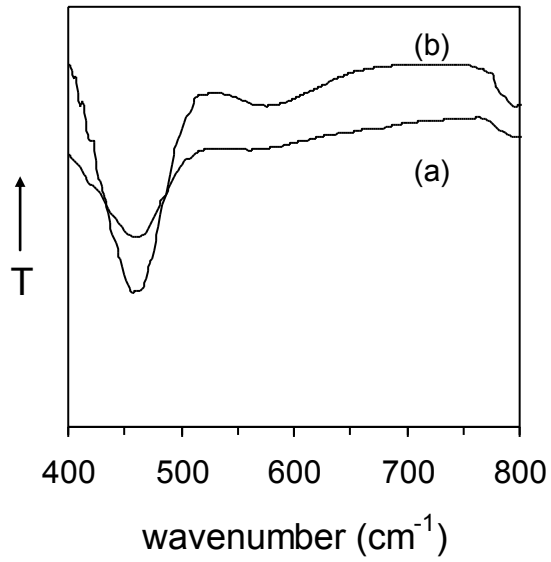

Figure 5.

J.P. Lourenço et al.
"Al- containing MCM-41 …"

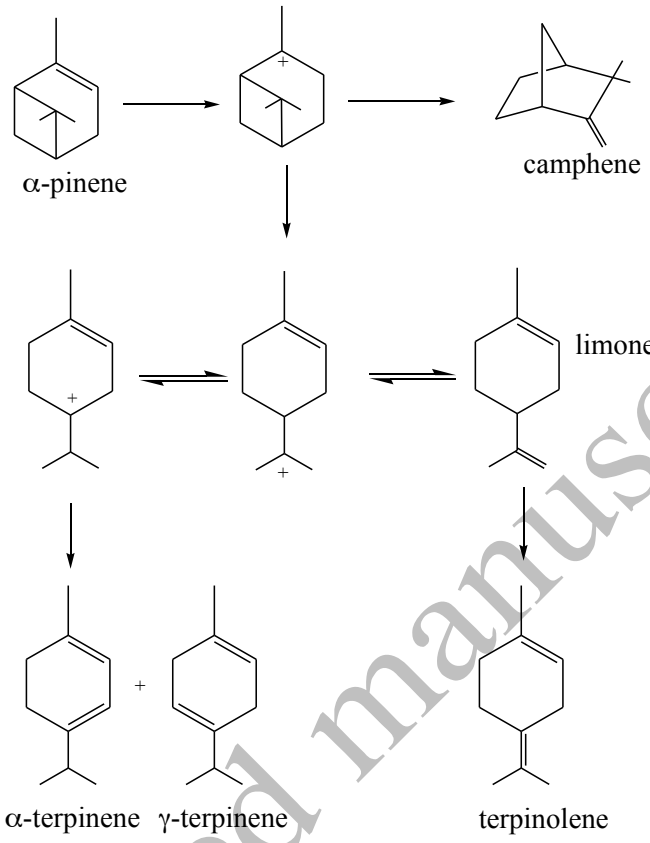

Figure 6.

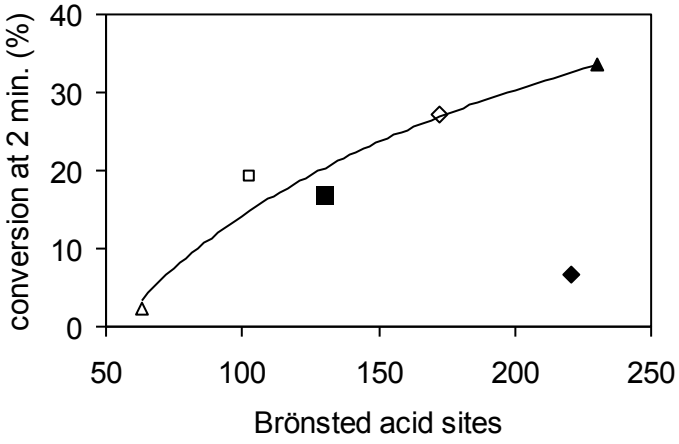

Figure 7.

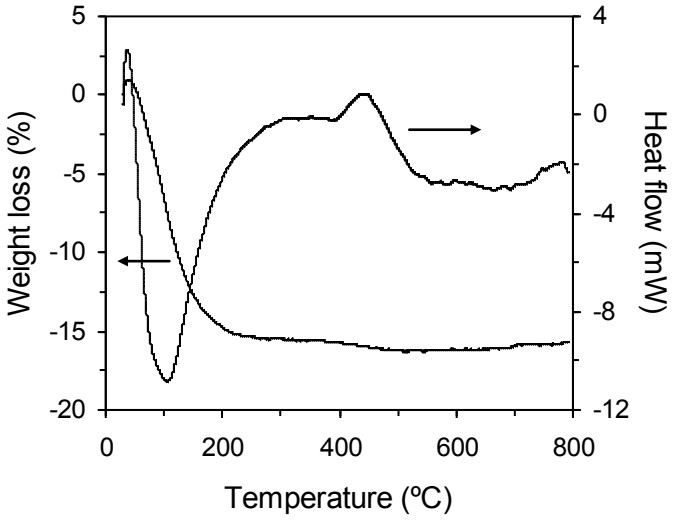

Figure 8.

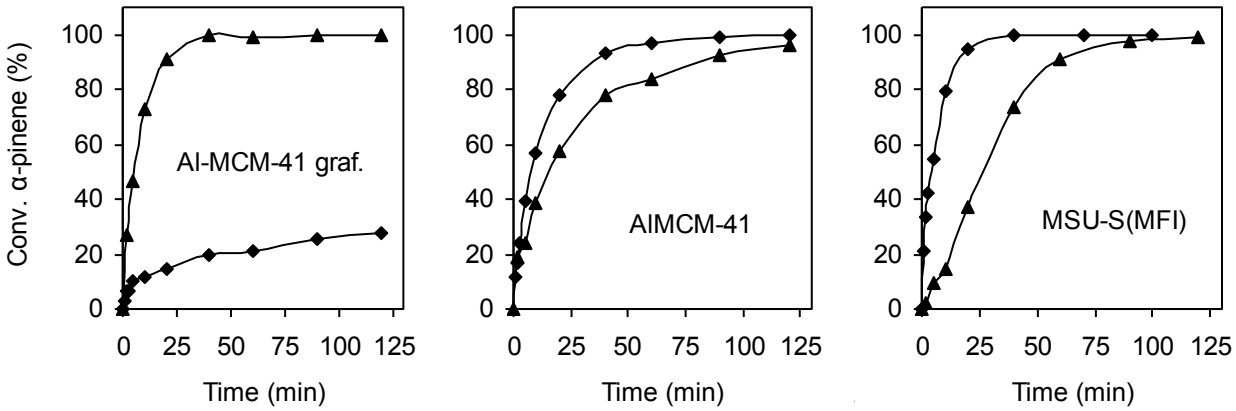

Figure 9.